2-1-2020

Antiviral inflammation during early pregnancy reduces placental and fetal growth trajectories

Kelly J. Baines
Schulich School of Medicine & Dentistry

Amanda M. Rampersaud
Schulich School of Medicine & Dentistry

Dendra M. Hillier
Schulich School of Medicine & Dentistry

Mariyan J. Jeyarajah
Schulich School of Medicine & Dentistry

Grace K. Grafham
Schulich School of Medicine & Dentistry

See next page for additional authors

The Journal of Immunology

Antiviral Inflammation during Early Pregnancy Reduces Placental and Fetal Growth Trajectories

Kelly J. Baines, Amanda M. Rampersaud, Dendra M. Hillier, Mariyan J. Jeyarajah, Grace K. Grafham, Genevieve Eastabrook, James C. Lacefield and Stephen J. Renaud

J Immunol 2020; 204:694-706; Prepublished online 27 December 2019;
doi: 10.4049/jimmunol.1900888
http://www.jimmunol.org/content/204/3/694

The Journal of Immunology is published twice each month by
The American Association of Immunologists, Inc.,
1451 Rockville Pike, Suite 650, Rockville, MD 20852

Print ISSN: 0022-1767 Online ISSN: 1550-6606.

Antiviral Inflammation during Early Pregnancy Reduces Placental and Fetal Growth Trajectories

Kelly J. Baines,* Amanda M. Rampersaud,* Dendra M. Hillier,* Mariyan J. Jeyarajah,* Grace K. Grafham,* Genevieve Eastabrook,[†,‡] James C. Lacefield,[§,¶,‖] and Stephen J. Renaud*[,‡]

Many viruses are detrimental to pregnancy and negatively affect fetal growth and development. What is not well understood is how virus-induced inflammation impacts fetal–placental growth and developmental trajectories, particularly when inflammation occurs in early pregnancy during nascent placental and embryo development. To address this issue, we simulated a systemic virus exposure in early pregnant rats (gestational day 8.5) by administering the viral dsRNA mimic polyinosinic:polycytidylic acid (PolyI:C). Maternal exposure to PolyI:C induced a potent antiviral response and hypoxia in the early pregnant uterus, containing the primordial placenta and embryo. Maternal PolyI:C exposure was associated with decreased expression of the maternally imprinted genes *Mest*, *Sfrp2*, and *Dlk1*, which encode proteins critical for placental growth. Exposure of pregnant dams to PolyI:C during early pregnancy reduced fetal growth trajectories throughout gestation, concomitant with smaller placentas, and altered placental structure at midgestation. No detectable changes in placental hemodynamics were observed, as determined by ultrasound biomicroscopy. An antiviral response was not evident in rat trophoblast stem (TS) cells following exposure to PolyI:C, or to certain PolyI:C-induced cytokines including IL-6. However, TS cells expressed high levels of type I IFNR subunits (*Ifnar1* and *Ifnar2*) and responded to IFN-α by increasing expression of IFN-stimulated genes and decreasing expression of genes associated with the TS stem state, including *Mest*. IFN-α also impaired the differentiation capacity of TS cells. These results suggest that an antiviral inflammatory response in the conceptus during early pregnancy impacts TS cell developmental potential and causes latent placental development and reduced fetal growth. ***The Journal of Immunology*****, 2020, 204: 694–706.**

Successful pregnancy requires a delicate balance between proinflammatory and anti-inflammatory pathways. Pathological inflammation disrupts this balance and is an underlying feature of a spectrum of prevalent pregnancy complications (1). In humans, it is difficult to discern whether inflammation is a cause or consequence of a compromised pregnancy, but circumstantial and epidemiological evidence implicate inflammation as a component of disease pathogenesis (2, 3). A direct link between inflammation and various pregnancy pathological conditions has been demonstrated in animal models in which dams are exposed to microbial products called pathogen-associated molecular patterns, resulting in changes in labor onset and alterations in fetal survival, growth, and developmental trajectories (4–7). However, the underlying mechanisms through which inflammation compromises fetal growth and development are still unknown.

Fetal growth restriction (FGR; also known as intrauterine growth restriction) is a serious pregnancy complication associated with failure of a fetus to grow to its full potential. Although an accepted definition and consensus diagnosis of FGR are lacking, it is generally defined as fetal weight below the 10th percentile for that population and gestational age while considering sex, race, and genetic growth potential (8). Identifying cases of morbid FGR versus healthy fetuses that are constitutionally small remains a significant problem. In general, FGR is one of the most important indicators of pregnancy outcome including prematurity, stillbirth, intrapartum fetal distress, hypoglycemia, and meconium aspiration pneumonia (9) as well as long-term growth impairments and permanent pulmonary, metabolic, endocrine, and neurobehavioral sequelae (10). FGR may be caused by multiple factors, including chromosomal aberrations, vascular abnormalities, and infections and in many cases is associated with inflammation as an underlying feature (11). In 40–50% of cases, the cause of FGR is idiopathic and attributed to maldevelopment or dysfunction of the placenta.

The placenta is the extraembryonic organ that ensures an adequate nutrient and gas supply for the fetus and as such is a critical regulator of fetal growth and development. The efficiency of transferring substrates needed for fetal growth, including oxygen,

*Department of Anatomy and Cell Biology, Schulich School of Medicine and Dentistry, University of Western Ontario, London, Ontario, Canada N6A 5C1; [†]Department of Obstetrics and Gynaecology, University of Western Ontario, London, Ontario, Canada N6H 5W9; [‡]Children's Health Research Institute, Lawson Health Research Institute, London, Ontario, Canada N6C 2V5; [§]Department of Electrical and Computer Engineering, School of Biomedical Engineering, University of Western Ontario, London, Ontario, Canada N6A 3K7; [¶]Department of Medical Biophysics, University of Western Ontario, London, Ontario, Canada N6A 3K7; and [‖]Robarts Research Institute, University of Western Ontario, London, Ontario, Canada N6A 5B7

ORCIDs: 0000-0002-3299-8659 (K.J.B.); 0000-0002-3189-089X (G.K.G.); 0000-0001-9184-2796 (G.E.); 0000-0002-9438-9189 (J.C.L.); 0000-0001-7257-5354 (S.J.R.)

Received for publication July 24, 2019. Accepted for publication November 28, 2019.

This work was supported by grants awarded by the Canadian Institutes of Health Research and the Preeclampsia Foundation Canada (to S.J.R.). K.J.B., A.M.R., and M.J.J. were supported in part through fellowships from the Children's Health Research Institute, London, Canada.

Address correspondence and reprint requests to Dr. Stephen J. Renaud, University of Western Ontario, MSB428, 1151 Richmond Street, London, ON N6A 5C1, Canada. E-mail address: srenaud4@uwo.ca

The online version of this article contains supplemental material.

Abbreviations used in this article: Ct, cycle threshold; *Cxcl10*, c-x-c motif ligand 10; *Dlk1*, δ-like noncanonical notch ligand 1; EDV, end diastolic velocity; FGR, fetal growth restriction; *Gcm1*, glial cells missing-1; GD, gestational day; IRF, IFN regulatory factor; *Mest*, mesoderm-specific transcript; PolyI:C, polyinosinic:polycytidylic acid; *Prl3b1*, prolactin family 3, subfamily b, member 1; PSV, peak systolic velocity; qRT-PCR, quantitative RT-PCR; RI, resistance index; *Rsad2*, radical SAM domain-containing 2; *Sfrp2*, secreted frizzled-related protein 2; TS, trophoblast stem; VTI, velocity time integral.

amino acids, glucose, and fatty acids, to the fetal circulation is dependent on placental size, morphology, and blood flow (12). Formation of the placenta begins shortly after blastocyst implantation and is contingent on proper proliferation and differentiation of trophoblast stem (TS) cells. TS cells are multipotent progenitor cells that specialize into heterogeneous trophoblast subtypes that form the bulk of the placenta and perform various functions required for fetal growth and pregnancy success. In humans, TS cells differentiate into extravillous trophoblasts, which direct maternal resources to the conceptus, and villous trophoblasts, which specialize in nutrient transfer between maternal and fetal blood. A similar dichotomous organization of the placenta occurs in rodents, in which junctional zone and labyrinth zone trophoblasts perform analogous functions to extravillous and villous trophoblasts, respectively (13). TS cell development and differentiation are adaptable and respond to changes in the surrounding environment, including cellular stress and changes in oxygen and nutrient delivery, providing the placenta a degree of plasticity during its early development to facilitate embryo survival during extrinsic challenges (14). Trophoblasts cultured from rodent blastocysts and ectoplacental cones alter their survival and differentiation potential in response to IFNs (15–18), indicating that inflammation may be an additional extrinsic challenge that can impact placental morphology and fetal growth.

To determine the effect of systemic inflammation on placental development and fetal growth, we injected rats with the viral mimic polyinosinic:polycytidylic acid (PolyI:C) during early pregnancy. PolyI:C is a synthetic analogue of dsRNA: a molecular pattern produced by many viruses, either as the genetic material for some RNA viruses or as an intermediate for viral RNA synthesis. PolyI:C is a ligand for the pattern recognition receptors TLR3, retinoid acid inducible gene-1 (RIG1), and melanoma differentiation-associated gene 5, which enables mammalian cells to detect the presence of viruses and initiate cellular antiviral responses, such as production of IFNs (19). Given the purported immune tolerance mechanisms evident within the conceptus during early pregnancy, we were uncertain whether an antiviral response would be evident at this site. We found that PolyI:C exposure during early pregnancy induced a robust antiviral response and hypoxia within the conceptus, close to the location of placental development. The antiviral response was associated with reduced placental and fetal size during middle and late pregnancy. Furthermore, we provide evidence that rat TS cells are responsive to IFN-α, and IFN-α exposure decreased expression of stem-related genes in these cells and reduced their differentiation capacity. Our results suggest that an IFN-mediated intrauterine antiviral response during early pregnancy causes transient placental dormancy by inhibiting TS cell developmental potential, resulting in smaller-than-normal placentas and fetuses.

Materials and Methods

Animals

Female (6–8 wk) and male (8–10 wk) Sprague Dawley rats were obtained from Charles River Laboratories and maintained in a 12-h light/12-h dark cycle with food and water available ad libitum. Females were cycled by daily inspection of cells within a vaginal lavage and mated when in proestrus with a fertile male. Gestational day (GD) 0.5 was defined as the day immediately following mating if spermatozoa were detected within the vaginal lavage. All protocols involving the use of rats were approved by the University of Western Ontario Animal Care and Use Committee.

Experimental protocol and tissue collection

In the first set of experiments, pregnant rats received PolyI:C (1, 5, or 10 mg/kg; Sigma-Aldrich) or sterile saline i.p. on GD8.5. Dams were sacrificed on GD13.5 to assess for fetal viability. Based on these results, 10 mg/kg PolyI:C was used in all subsequent experiments because there was no difference in litter size or number of resorptions with any of the doses tested, and it is a dose that has been previously used in pregnant dams to elicit long-term metabolic and neurodevelopmental problems in offspring (20–24). For experiments in which fetal and placental growth were analyzed, dams were sacrificed on GD8.5 (6 h after maternal saline or PolyI:C injection), GD13.5 (5 d after maternal saline or PolyI:C injection), or GD18.5 (10 d after maternal saline or PolyI:C injection) using mild carbon dioxide inhalation until respiratory failure, followed by cardiac puncture or decapitation. For tissues collected on GD8.5, whole conceptuses (containing decidua, placenta, and embryo) were isolated and either snap-frozen in liquid nitrogen or fixed in 10% neutral buffered formalin. For analysis of placental and fetal weights on GD13.5 or GD18.5, uterine horns were dissected to isolate whole conceptuses, preserved in 10% neutral buffered formalin for 24 h, and then dissected to isolate and independently weigh the fetus and placenta. Preservation was used to enhance the structural integrity of fetal tissue, particularly for tissues isolated on GD13.5, and ensure that residual fetal membranes were completely removed. Fetal weights were consistent between fresh and fixed specimens. Fetal crown-rump length was also measured using a digital caliper. For cryosections, whole conceptuses were placed in dry ice–cooled heptane and stored at −80°C until sectioned. For paraffin-embedded sections, whole conceptuses were fixed in 10% neutral buffered formalin for at least 24 h, then transferred to 70% ethanol and stored at 4°C prior to sectioning.

RT-PCR

RNA was extracted from tissue by homogenizing in TRIzol (Thermo Fisher Scientific). The aqueous phase was then diluted with 70% ethanol, placed on RNeasy columns (Qiagen), treated with DNase I, and purified. RNA was extracted from cells by lysing in TRIzol and proceeding as directed by the manufacturer. cDNA was generated from purified RNA (50 ng/μl) using High Capacity cDNA Reverse Transcription kit (Thermo Fisher Scientific), diluted 1:10, and used for conventional RT-PCR or quantitative RT-PCR (qRT-PCR). Conventional RT-PCR was conducted using primers described in Table I, and DreamTaq DNA Polymerase (Thermo Fisher Scientific) to amplify cDNA. Cycling conditions involved an initial holding step (95°C for 3 min), followed by 34 cycles of PCR (95°C for 30 s, 55°C for 30 s, and 72°C for 1 min), and a final elongation phase at 72°C for 5 min. PCR products were resolved on 2% agarose gels and imaged using a ChemiDoc imaging system (Bio-Rad Laboratories). For qRT-PCR, cDNA was mixed with SensiFAST SYBR green PCR Master Mix (FroggaBio) and primers described in Table I. A CFX Connect Real-Time PCR system (Bio-Rad Laboratories) was used for amplification and fluorescence detection. Cycling conditions were as follows: an initial holding step (95°C for 3 min), followed by 40 cycles of two-step PCR (95°C for 10 s, 60°C for 45 s), then a dissociation step (65°C for 5 s and a sequential increase to 95°C). Relative mRNA expression was calculated using the comparative cycle threshold (Ct) (ΔΔCt) method. The geometric mean of Ct values obtained from amplification of five constitutively expressed genes (*Rn18s*, *Ywhaz, Eef2, Gapdh*, and *Actb*) was used as reference RNA. Ct values from each of these genes were stable among the conditions tested.

Ultrasound

Ultrasound imaging and Doppler waveform recordings were used to compare blood flow patterns in the maternal uterine artery and fetal umbilical vessels. Dams were anesthetized with inhaled isoflurane (4% induction, 1–3% maintenance). Body temperature was maintained at 36–38°C with a heating pad. Heart rate and respiratory physiology were monitored throughout the imaging procedure. Hair was removed from the abdomen by shaving, followed by application of a depilatory cream, after which a coupling gel (37°C) was applied. Rats were imaged transcutaneously using a preclinical ultrasound imaging system (model Vevo 2100; FujiFilm VisualSonics) coupled with MS-250 (20 MHz, uterine artery) and MS-400 (30 MHz, umbilical artery) MicroScan transducers. The transducer beam angle was set to <45° for all measurements. Doppler waveforms were obtained from the uterine artery near the utero-cervical junction and from the umbilical artery spanning the fetal–placental junction. Peak systolic velocity (PSV) and end diastolic velocity (EDV) were manually measured from three sequential cardiac cycles, and data were averaged. The resistance index (RI) (RI = [PSV − EDV]/PSV) was then calculated to quantify the resistance of arterial blood velocity waveforms. Uterine artery measurements were recorded from nine dams per group; umbilical artery measurements were conducted in at least two conceptuses from each of these dams. The duration of anesthesia was limited to no more than 45 min. During this time, maternal and fetal circulatory parameters were not noticeably affected.

Western blotting

Protein expression was evaluated by Western blotting. Total protein in tissues was isolated by homogenizing snap-frozen GD8.5 conceptuses in radioimmunoprecipitation assay lysis buffer (50 mM Tris, 150 mM NaCl, 1% Nonidet P-40, 0.5% sodium deoxycholate, 0.1% SDS, pH 7.2) supplemented with protease inhibitor mixture (Sigma-Aldrich) and then sonicated (Sonic Dismembrator Model 100; Thermo Fisher Scientific). A modified bicinchoninic acid assay (Bio-Rad Laboratories) was used to measure total protein concentrations. Approximately 25 μg of tissue lysates were mixed with 4× loading buffer (final volume: 62.5 mM Tris, pH 6.8, 2% SDS, 10% glycerol, 0.025% bromophenol blue, 50 mM DTT), boiled for 5 min, and subjected to SDS-PAGE. Proteins were then transferred to polyvinylidene difluoride (PVDF) membranes, blocked with 3% BSA in TBS containing 0.1% Tween-20, and probed with primary Abs specific for STAT1 (catalog no. 14994, 1:1000; Cell Signaling Technology), VIPERIN (catalog no. MABF106, 1:1000; Sigma-Aldrich), and IFN regulatory factor (IRF) 1 (catalog no. 8478, 1:1000; Cell Signaling Technology). Expression of GAPDH (catalog no. 5174, 1:1000; Cell Signaling Technology) was used as a loading control. Following incubation with species-appropriate, infrared-conjugated secondary Abs (Cell Signaling Technology), protein signals were detected using a LI-COR Odyssey imaging system (LI-COR Biotechnology).

Immunohistochemistry

Frozen conceptuses were embedded in Optimal Cutting Temperature compound and cryosectioned at 10-μm thickness. Sections were fixed in 10% neutral buffered formalin, permeabilized using 0.3% Triton-X and 1% BSA in PBS, and blocked in 10% normal goat serum (Thermo Fisher Scientific). Sections were immersed in primary Abs specific for cytokeratin (catalog no. 628602, 1:400; BioLegend) and vimentin (catalog no. MA5-11883, 1:50; Invitrogen) overnight at 4˚C. After washing, sections were immersed in species-appropriate biotin-conjugated secondary IgG Abs followed by Vectastain ABC Elite reagent (Vector Laboratories), and color was developed using 3-amino-9-ethylcarbazole (AEC) red (Thermo Fisher Scientific). Sections were counterstained with Gill No. 1 hematoxylin (Sigma-Aldrich) and mounted using Fluoromount-G mounting medium (SouthernBiotech). Images were acquired using a Nikon ECLIPSE Ni Series microscope equipped with a Ds-Qi2 camera. Placental sections that were immunostained using vimentin (which is detectable in labyrinth zone and uterine tissue but not in junctional zone and is therefore useful for demarcating different placental zones) were subjected to morphometric analysis using ImageJ software (25). The mean thickness of the conceptus, placenta (junctional zone and labyrinth zone), and each zone was calculated following three independent measurements within the middle of the placenta. The mean area of each placenta and zone was calculated following three independent measurements of the perimeter. All measurements were conducted by two researchers who were blinded to the experimental treatments, and results between observers were averaged.

To detect localization of perforin-containing cells on GD8.5, whole conceptuses were collected, fixed in 10% neutral buffered formalin, embedded with paraffin, and sectioned at 5-μm thickness. Sections were dewaxed in Histo-clear and rehydrated using increasing dilutions of ethanol. Formaldehyde crosslinks were broken by immersing sections in a retrieval solution (Reveal Decloaker; BioCare Medical) heated to 95˚C for 20 min. Sections were then permeabilized using 0.3% Triton-X and 1% BSA in PBS and blocked in 10% normal goat serum. Samples were immersed in primary Ab specific for rat perforin (catalog TP251, 1:400; Torrey Pines Biolabs) overnight at 4˚C, followed by Alexa 555–conjugated anti-rabbit secondary Ab for 1 h at room temperature. Sections were then immersed in an Ab specific for cytokeratin (BioLegend) for 1 h, then exposed to Alexa 488–conjugated anti-mouse secondary Abs, and mounted using Fluoromount-G. Images were acquired using a Nikon ECLIPSE Ni Series microscope equipped with a Ds-Qi2 camera. Sections were subjected to localization analysis using ImageJ software (25). The distance between the bulk of perforin-positive cells and the tip of the ectoplacental cone was measured in arbitrary units (pixels) and calculated relative to the length of the ectoplacental cone.

Detection of hypoxia

To assess hypoxia in uterine and placental tissue after maternal PolyI:C exposure, immunohistochemical staining for pimonidazole was performed. Pimonidazole covalently binds to thiol groups in proteins of cells exposed to hypoxia ($pO_2 < 10$ mm Hg). Pimonidazole adducts can then be detected immunohistochemically to denote tissue areas exposed to hypoxic conditions.

Rats were i.p. injected with pimonidazole hydrochloride (hypoxyprobe-1, 60 mg/kg; Natural Pharmacia) 2.5 h before sacrifice. After euthanasia, whole conceptuses were collected, fixed in 10% neutral buffered formalin, and embedded with paraffin. Paraffin-embedded tissues were then sectioned at 5-μm thickness. Sections were dewaxed in Histo-clear and rehydrated using increasing dilutions of ethanol. Formaldehyde crosslinks were broken by immersing sections in Reveal Decloaker, as described above. Endogenous peroxidases were then inhibited using 3% hydrogen peroxide in PBS, and tissues were blocked in 10% normal goat serum. Sections were incubated in hypoxyprobe-1 mouse mAb (clone 4.3.11.3, 1:50; Natural Pharmacia), followed by biotin-conjugated anti-mouse secondary IgG Ab. Following wash, samples were then immersed in Vectastain (Vector Laboratories) for 30 min at room temperature, and color was developed using AEC red (Thermo Fisher Scientific). Samples were counterstained with Gill No. 1 hematoxylin (Sigma-Aldrich), mounted, and imaged as above.

Rat TS cell cultures

Blastocyst-derived rat TS cells (26) were used to evaluate the effects of PolyI:C, or selected PolyI:C-induced cytokines, on trophoblast cell behavior. Rat TS cells were generously provided by Michael Soares (University of Kansas Medical Center, Kansas City, KS). Cells were cultured in RPMI 1640 media (Life Technologies) supplemented with 20% (v/v) FBS (Life Technologies), 100 μM 2-ME (Sigma-Aldrich), 1 mM sodium pyruvate (Sigma-Aldrich), 50 μM penicillin, 50 U/ml streptomycin, fibroblast growth factor 4 (25 ng/ml; R&D Systems), and heparin (1 μg/ml; Sigma-Aldrich). A total of 70% of the media was preconditioned by mitomycin C–treated mouse embryonic fibroblasts prior to being added to rat TS cells. PolyI:C (50 μg/ml), recombinant rat IFN-α1 (100 U/ml or 1000 U/ml; R&D Systems), recombinant rat IL-6 (IL-6, 20 ng/ml; PeproTech), or recombinant rat IFN-γ (100 U/ml; PeproTech) was added to TS cells for 24 h. Transfection of PolyI:C (50 μg/ml) into rat TS cells was conducted using lipofectamine 2000 (Thermo Fisher Scientific). To determine the effect of IFN-α on trophoblast differentiation, rat TS cells were cultured for 3 d as above but without mouse embryonic fibroblast-conditioned media, fibroblast growth factor 4, activin A, or heparin and in the presence or absence of recombinant rat IFN-α1 (1000 U/ml). Media were replaced daily.

Immunocytochemistry and EdU incorporation

Cells were fixed in 4% paraformaldehyde, permeabilized using 0.3% Triton-X, and blocked using 10% normal goat serum (Life Technologies). Cells were then immersed in anti-phospho-histone H3 Ab (1:1000, catalog no. 3377P; Cell Signaling Technology), followed by goat anti-rabbit Alexa Fluor 488–conjugated secondary Ab. Nuclei were then counterstained using DAPI (Thermo Fisher Scientific). For EdU, rat TS cells were treated with 10 μM EdU (ClickiT EdU Proliferation Kit; Thermo Fisher Scientific) for 6 h, followed by fixation as above. Detection of EdU was performed as per the manufacturer's instructions, and nuclei were detected by counterstaining with Hoechst. Cells were imaged with a Zeiss Axio fluorescence microscope. The total number of cells, and the number positive for phospho-histone H3 or EdU, was then counted in three random nonoverlapping fields of view per well. The percentage of phospho-histone H3 and EdU-positive cells was then calculated by dividing the total number of positive cells by the total number of cells, then multiplying by 100.

Statistical analysis

Values are expressed as mean ± SEM. Unless indicated otherwise, statistical significance was analyzed by unpaired *t* test when comparing two groups and one-way ANOVA with Tukey multiple comparisons test when comparing three or more groups. All statistical tests were two sided, and differences were considered significant when $p \leq 0.05$. All animal experiments were conducted with a minimum of three dams. The specific number of dams and conceptuses analyzed is indicated in the figure legends.

Results

Maternal PolyI:C exposure triggers a potent antiviral response within the conceptus during early pregnancy

PolyI:C is an analogue of dsRNA, which is a molecular pattern associated with viral infection and a well-known inducer of antiviral immune responses. The pregnant uterus and fetal–placental unit are considered immune-privileged sites, so our first goal was to determine whether systemic PolyI:C administration to pregnant

dams elicited an antiviral response within the conceptus (referring to decidualized uterine tissue along with primordial placenta and embryo). Compared with pregnant rats administered saline, expression of genes encoding various antiviral factors was increased within the conceptus 6 h after injecting pregnant rats with 10 mg/kg PolyI:C, including IFN-α (*Ifna,* 3.3-fold increase), *Il6* (11-fold increase), *Il1a* (17-fold increase), *Il1b* (6-fold increase), c-x-c motif ligand (Cxcl) 10 (*Cxcl10*; 323-fold increase), IRF 7 (*Irf7*, 22-fold increase), IDO (*Ido1*, 221-fold increase), radical SAM domain-containing 2 (*Rsad2*; 166-fold increase), and *Tlr3* (5-fold increase, Fig. 1A, all $p < 0.05$, primer sequences provided in Table I). Myxovirus resistance 1 (*Mx1*), which is an IFN-inducible gene encoding a dynamin-like GTPase that confers an antiviral state against a wide range of RNA viruses (including influenza A) and some DNA viruses, was also highly upregulated in the conceptus following PolyI:C exposure (386-fold increase, Fig. 1A, $p < 0.05$). A similar robust antiviral response was detected when transcript levels were evaluated within isolated decidua following maternal PolyI:C exposure.

Next, we determined whether PolyI:C altered expression of select proteins associated with antiviral immune responses. PolyI:C exposure to pregnant dams caused a rapid increase in RSAD2 (also known as VIPERIN, which is a multifunctional protein that inhibits viral processes) in the conceptus 2, 6, and 12 h after injection and increased IRF1 expression 2 and 6 h after injection. Both VIPERIN and IRF1 are directly and rapidly activated by both PolyI:C and IFNs and contribute to the cellular antiviral state (27). Injection of PolyI:C also increased expression of STAT1 in the conceptus 12 and 24 h after maternal exposure (Fig. 1B). The relatively longer time required for increased STAT1 expression in comparison with VIPERIN and IRF1 likely relates to the time required for protein stabilization and accumulation following activation (28). Collectively, these data indicate that maternal exposure to PolyI:C during early pregnancy provokes a robust antiviral response near the site of placental and embryonic development.

We next assessed expression of nine maternally imprinted genes associated with embryonic and placental growth and development (29). In pregnant rats exposed to PolyI:C, we observed decreased expression of mesoderm-specific transcript (*Mest,* 4-fold decrease), a gene highly associated with placental growth, as well as secreted frizzled-related protein 2 (*Sfrp2*; 2.4-fold decrease) and δ-like noncanonical notch ligand 1 (*Dlk1*, 1.7-fold decrease, Fig. 1C, all $p < 0.05$). Expression of *Dio3* appeared to be decreased, although it did not reach statistical significance ($p = 0.10$, not shown). No change in expression of MAGE family member L2 (*Magel2*; not shown), paternally expressed gene 3 (*Peg3*), paternally

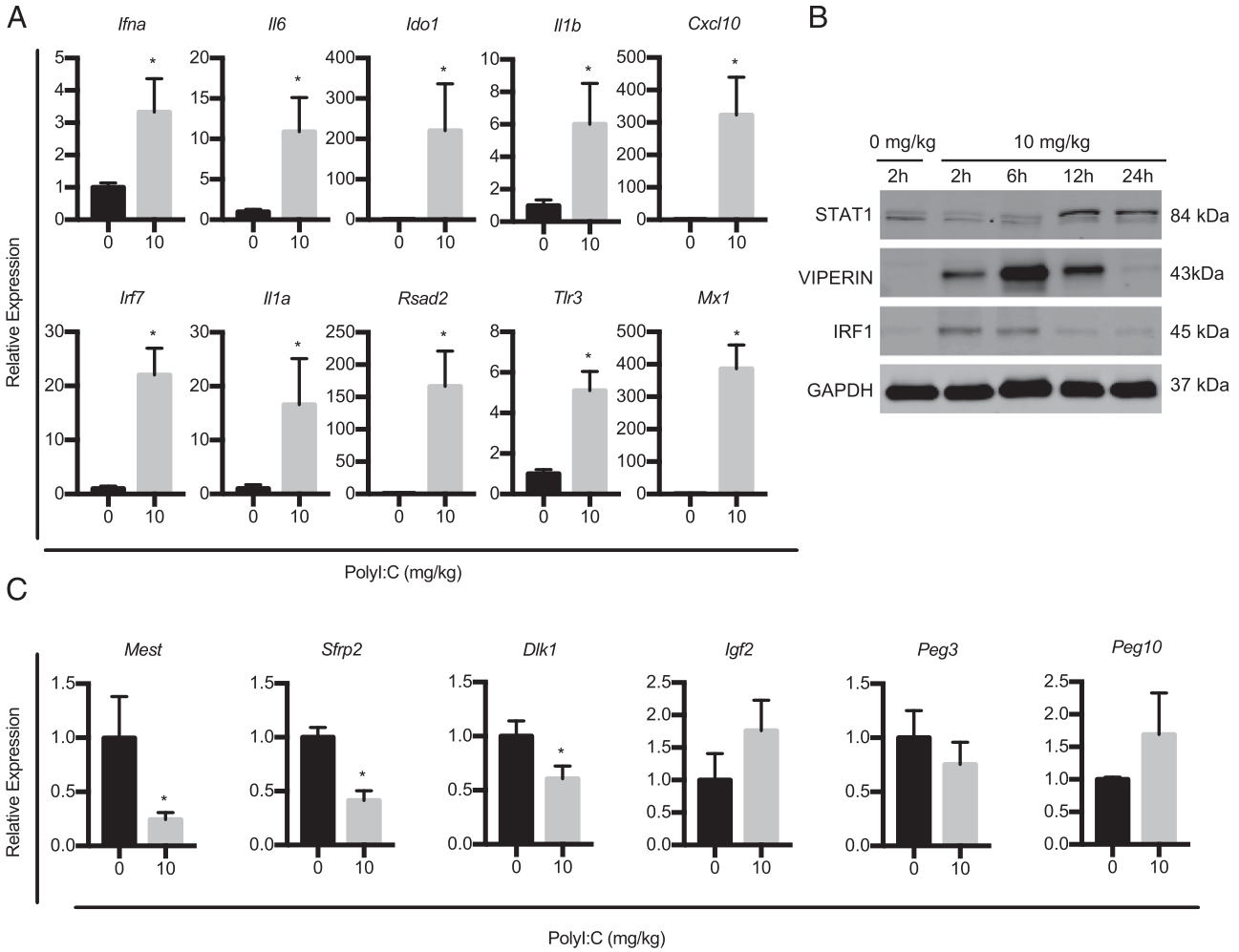

FIGURE 1. Exposure of pregnant rats to PolyI:C elicits a robust antiviral response in the conceptus. RNA was isolated from the conceptus (containing decidua, primordial placenta, and embryo) 6 h following maternal injection of 10 mg/kg PolyI:C or saline (0 mg/kg PolyI:C) on GD8.5. (**A**) Expression of genes associated with antiviral responses after saline or PolyI:C exposure. (**B**) Protein levels of STAT1, VIPERIN, IRF1, and GAPDH are shown 2, 6, 12, and 24 h following maternal PolyI:C exposure (10 mg/kg) or 2 h following maternal saline exposure (0 mg/kg). Uncropped images of Western blots are provided in Supplemental Fig. 3. (**C**) Expression of maternally imprinted genes associated with fetal and placental growth after saline or PolyI:C exposure. Results represent means ± SEM. Data significantly different ($p < 0.05$) from controls are indicated by an asterisk (*) ($n = 9$ from three dams per group).

Table I. List of primers used for RT-PCR

Gene	Accession Number	Forward Sequence	Reverse Sequence	Size (kb)
Actb	NM_031144.3	5′-AGCCATGTACGTAGCCATCC-3′	5′-CTCTCAGCTGTGGTGGTGAA-3′	226
Cdx2	NM_023963.1	5′-GAGCACGGACACTGTGAGAA-3′	5′-AGAAGCCCCAGGAATCACTT-3′	200
Cxcl10	NM_139089.1	5′- TGTCCGCATGTTGAGATCAT-3′	5′-GGGTAAAGGGAGGTGGAGAG-3′	202
Dio3	NM_017210.4	5′- GCCTCTACGTCATCCAGAGC-3′	5′-GCCCACCAATTCAGTCACTT-3′	169
Dlk1	NM_053744.1	5′-GAGCTGGCGGTCAATATCAT-3′	5′-GCATAGAGGGAGCTGTGAGG-3′	149
Ddx58	NM_001106645.1	5′-TCCTCCCACCTGTTTGAGAC-3′	5′-ACAAGCCATGTTAGGGGATG-3′	200
Eef2	NM_017245.2	5′-CGCTTCTATGCCTTCGGTAG-3′	5′-GTAGTGATGGTGCCGGTCTT-3′	234
Gapdh	NM_017008.4	5′- AGACAGCCGCATCTTCTTGT-3′	5′-CTTGCCGTGGGTAGAGTCAT-3′	206
Gcm1	NM_017186.2	5′-CCTCAATGATTGCCTGTCCT-3′	5′-TCCAGGTTTGTGCTTCATCA-3′	199
Id2	NM_013060.3	5′-TGAAAGCCTTCAGTCCGGTG-3′	5′-GAGCTTGGAGTAGCAGTCGT-3′	137
Ido1	NM_023973.1	5′- CGTGGATCCAGACACCTTTT-3′	5′-GGCTGGAGGCATGTACTCTC-3′	246
Ifna	NM_001014786.1	5′-GGTGGTGGTGAGCTACTGGT-3′	5′-TTGAGCCTTCTGGATCTGCT-3′	192
Ifnar1	NM_001105893.1	5′- ATTACGTGTTCTCCCCACCA-3′	5′-CGATTCTCCTCTCCAGCAAC-3′	156
Ifnar2	XM_006248107.3	5′-TGGCCCACAAATGTTCTTCT-3′	5′-GTGCACCCTAATGCTGTCCT-3′	182
Igf2	NM_001190162.1	5′-CGGACGACTTCCCCAGATAC-3′	5′-CTGAACGCTTCGAGCTCTTT-3′	142
Il1b	NM_031512.2	5′-AGGCTTCCTTGTGCAAGTGT-3′	5′-TGAGTGACACTGCCTTCCTG-3′	228
Il6	NM_012589.2	5′-GCCAGAGTCATTCAGAGCAA-3′	5′-CATTGGAAGTTGGGGTAGGA-3′	99
Il6r	NM_017020.3	5′-AGGGTGTCTGCTTCCTGCTA-3′	5′-TTGTGAAAAGGCAAGCTCCT-3′	232
Irf7	NM_001033691.1	5′-CCTCTGCTTTCTGGTGATGC-3′	5′-GCGCTCAGTCATCAGAACTG-3′	206
Isg15	NM_001106700.1	5′-GCCATGACCTGGAACCTAAA-3′	5′-CTGCCTGATAAGGGCAACAC-3′	188
Isg20	NM_001008510.1	5′-TCTGAAAGGCAAGCTGGTG-3′	5′-TGGACGTGTCGTAGATGGTG-3′	94
Magel2	XM_001054803.6	5′-TCCAGCCTGCCTCTACTGAT-3′	5′-GACTTGGAAGCCTCTGCATC-3′	234
Mest	NM_001009617.1	5′-CCATCGTCCTCTCCTTCTCC-3′	5′-TCCCGTCATTGTTGCGAATC-3′	182
Mx1	NM_001271058.1	5′-CCTGAGGTAAGGCTGTGGAA-3′	5′-AATACGGCCCCACAAAACAC-3′	210
Plagl1	NM_012760.3	5′-GGTGCTGCCTTTTCAGAGTC-3′	5′-CCACACTCAGTCTTGGAGCA-3′	244
Peg3	NM_001304816.1	5′-CAGAATGAACTGGCAGACGA-3′	5′-GGTGTAGGAGGGCCCATATT-3′	188
Peg10	XM_008762737.1	5′-GTTGACCGTGTCCGTGTATG-3′	5′-GACGTCTGATCTTGCGTTTG-3′	183
Pgf	NM_053595.2	5′-AGACGACAAAGGCAGAAAGG-3′	5′-TCTCCTCTGAGTGGCTGGTT-3′	119
Prl3b1	NM_012535.3	5′-ACCTGGAGCTGTTGGAAGTG-3′	5′-GACAGGGATGGCTACTCAGC-3′	198
Rn18s	NM_046237.1	5′-GCAATTATTCCCCATGAACG-3′	5′-GGCCTCACTAAACCATCCAA-3′	137
Rsad2	NM_138881.1	5′-GGGATGCTAGTGCCTACTGC-3′	5′-CTGAGTCTCCTTGGGCTCAC-3′	174
Sfrp2	NM_001276712.1	5′-TGTCCGATAGGGACCTGAAG-3′	5′-CGAGAAGCCACTCCACTAGG-3′	231
Tlr3	NM_198791.1	5′-GGTGGCCCTTAAAAGTGTGG-3′	5′-GGTTTGCGTGTTTCCAGAGT-3′	184
Vegfa	NM_001110333.2	5′-CAATGATGAAGCCCTGGAGT-3′	5′-TTTCTTGCGCTTTCGTTTTT-3′	210
Ywhaz	NM_013011.3	5′-TTGAGCAGAAGACGGAAGGT-3′	5′-CCTCAGCCAAGTAGCGGTAG-3′	200

expressed gene 10 (*Peg10*), or insulin-like growth factor 2 (*Igf2*) was detected in the conceptus after maternal exposure to PolyI:C (Fig. 1C). Transcript levels of another maternally imprinted gene, PLAG1-like zinc finger 1 (*Plagl1*), did not meet the threshold detection levels (Ct $>$ 30 cycles).

Maternal PolyI:C exposure is associated with acute hypoxia within the conceptus during early pregnancy

To assess whether maternal administration of PolyI:C increased tissue hypoxia within the conceptus, immunohistochemical detection of pimonidazole was used. Sections of the conceptus collected from saline-injected dams showed moderate levels of pimonidazole immunoreactivity, indicative of hypoxic regions proximate to the primordial placenta (Fig. 2). In comparison, following maternal PolyI:C administration, pimonidazole immunoreactivity was noticeably more intense, suggesting that PolyI:C administration altered tissue oxygenation (Fig. 2). Likewise, maternal administration of PolyI:C was also associated with a 1.7-fold increase in hypoxia-inducible factor 1 α (*Hif1a*) transcript levels, and a 2-fold increase in transcript levels of the hypoxia-inducible gene *Vegfa* within conceptuses (Fig. 2C, $p < 0.05$).

The pregnant uterus contains an abundant population of perforin-containing uterine NK cells. PolyI:C alters the activation of uterine NK cells (30, 31), so we sought to examine whether maternal PolyI:C exposure during early pregnancy alters localization of these cells. In dams injected with saline, perforin-containing cells were abundant within the decidua, but few cells were detectable close to the site of placental development. Following injection of PolyI:C, there appeared to be an accumulation of perforin-positive cells adjacent to the nascent placenta in some conceptuses. However, the effect was variable, and we were unable to detect a statistically significant difference in the distance separating perforin-positive cells from the nascent placenta (Supplemental Fig. 1). Collectively, these results indicate that maternal PolyI:C exposure during early pregnancy alters the decidual microenvironment during development of the nascent placenta and embryo.

Maternal PolyI:C exposure during early pregnancy is associated with reduced fetal weight at mid and late gestation

After determining that maternal PolyI:C administration during early pregnancy triggered a robust antiviral response and tissue hypoxia within the conceptus, our next goal was to examine fetal growth and survival 5 and 10 d after maternal exposure to PolyI:C. On GD13.5, average fetal weight was decreased by 10% in dams exposed to PolyI:C in early pregnancy compared with those exposed to saline (Fig. 3A, $p < 0.05$). Similarly, fetal crown-rump length was reduced by 9% following maternal PolyI:C exposure (Fig. 3B, $p < 0.05$). Because fetal growth is often referenced to percentiles for a given gestational age and babies smaller than the 10th centile are typically considered small for gestational age, we characterized the distribution of control GD13.5 fetuses using the saline-treated group to generate percentiles. Fetuses falling below the 10th percentile (0.068 g weight; 8.17 mm crown-rump length) were considered FGR. Strikingly, maternal PolyI:C exposure during early pregnancy caused 73% of fetuses to fall below the FGR threshold in weight and 52% to fall below the FGR threshold in crown-rump length (Fig. 3A, 3B, $p < 0.05$). On GD18.5, fetal body weight and crown-rump length remained smaller in dams exposed to PolyI:C, although these effects were more modest in

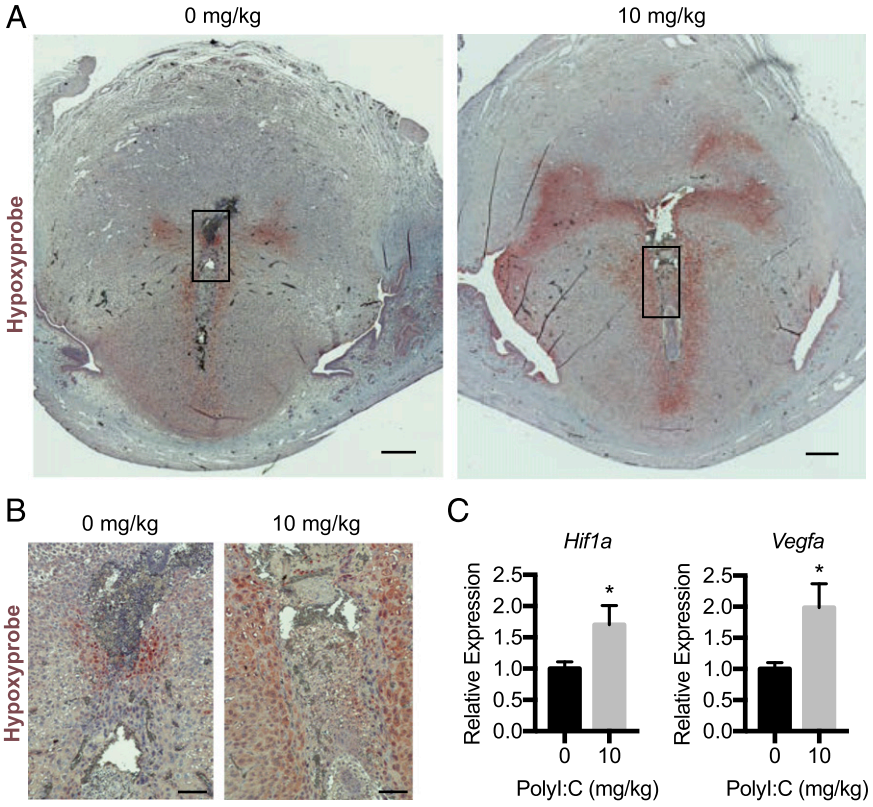

FIGURE 2. Detection of hypoxia in the conceptus following maternal exposure to PolyI:C. (**A**) Hypoxia was detected in sections of the conceptus collected 6 h following maternal PolyI:C (10 mg/kg) or saline (0 mg/kg) exposure using hypoxyprobe. The black boxes surround the ectoplacental cone (part of the primordial placenta), and a higher magnification image is shown in (**B**). Scale bar in (A), 1000 μm. Scale bar in (B), 100 μm. (**C**) Transcript levels of *Hif1a* and *Vegfa* 6 h following saline or PolyI:C exposure. Results represent means ± SEM. Data significantly different ($p < 0.05$) from controls are indicated by an asterisk (*) ($n = 9$ from three dams per group).

comparison with that which was observed on GD13.5 (decreased by 9 and 2% compared with saline-treated dams, respectively, Fig. 3C, 3D, $p < 0.05$), suggesting that these fetuses had some degree of catch-up growth. Using the same percentile strategy to characterize distribution of control GD18.5 fetuses, we observed a greater percentage of fetuses with weights and crown-rump lengths below the 10th centile when dams were exposed to PolyI:C 10 d earlier (43% in weight, 16% in crown-rump length, Fig. 3C, 3D, $p < 0.05$). In line with the smaller overall fetal size, maternal PolyI:C exposure was associated with smaller fetal liver weights (9% decrease, $p < 0.05$) and fetal brain weights (10% decrease, $p < 0.05$) compared with saline-injected dams (Fig. 3E). Surprisingly, we did not observe any significant difference in litter size, as well as number of viable or resorbed fetuses, indicating that PolyI:C did not affect fetal survival (Fig. 3F). Thus, maternal exposure to PolyI:C during early gestation is associated with delayed or impaired fetal growth at mid and late gestation without affecting viability.

Maternal PolyI:C exposure results in smaller placentas

Proper development of the placenta is fundamental for supporting fetal growth throughout pregnancy. Because maternal PolyI:C exposure induced a potent antiviral response within the conceptus and was associated with reduced fetal growth, we next evaluated the effect of PolyI:C on placental growth and development. As illustrated schematically in Fig. 4A, the rodent placenta is composed of three distinct zones. The labyrinth zone is situated closest to the chorionic plate (and, hence, the fetus) and is specialized to promote nutrient and gas transfer between maternal and fetal blood. The middle layer is the junctional zone, which forms the interface between maternal and fetal tissue. The maternal portion of the placenta includes the decidua and mesometrial triangle, which contain a variety of cell types (e.g., stromal cells, blood vessels, leukocytes) that support placentation and pregnancy outcome.

We did not observe a noticeable difference in the composition of the maternal portion of the placenta 5 d following exposure to PolyI:C. Specifically, there was no evident change in the area or thickness of the decidua or mesometrial triangle, number or localization of NK cells, blood vessels, or the depth of trophoblast invasion between saline- or PolyI:C-exposed dams on GD13.5. However, in dams exposed to PolyI:C on GD8.5, average placental weight, area, and thickness were reduced on GD13.5 (15, 10, and 8% decreased compared with saline-treated dams, respectively; Fig. 4, $p < 0.05$ for all), concomitant with reduced area and thickness of the junctional zone (12 and 17%, respectively, Fig. 4, $p < 0.05$) and labyrinth zone (14 and 6%, Fig. 4, $p < 0.05$). Interestingly, the effects of maternal PolyI:C exposure on placental structure were transient, as there were no differences in placental weights, zonal areas, or thicknesses on GD18.5 (Supplemental Fig. 2). Collectively, these results suggest that PolyI:C exposure during early pregnancy is associated with a transient impairment or delay in development of the fetal components of the placenta.

To assess whether placental hemodynamics were altered on GD13.5 following maternal PolyI:C exposure, ultrasound biomicroscopy was performed to measure blood flow in uterine and umbilical vasculature. There were no statistically significant differences in blood flow through the uterine artery 5 d after maternal exposure to PolyI:C, as determined by average PSV, EDV, RI, and velocity time integral (VTI) (Fig. 5A). In the umbilical artery, there was no difference detected when measuring EDV, RI, heart rate, and VTI. We did note a modest 23% increase in PSV 5 d after maternal exposure to PolyI:C (Fig. 5B, $p < 0.05$), although in the absence of a statistical difference in other umbilical vessel parameters, we are unable to conclude whether this difference has important implications for placental function and fetal growth (32). Collectively, these results demonstrate efficient hemodynamics of the placenta following early gestational exposure to PolyI:C despite their smaller size.

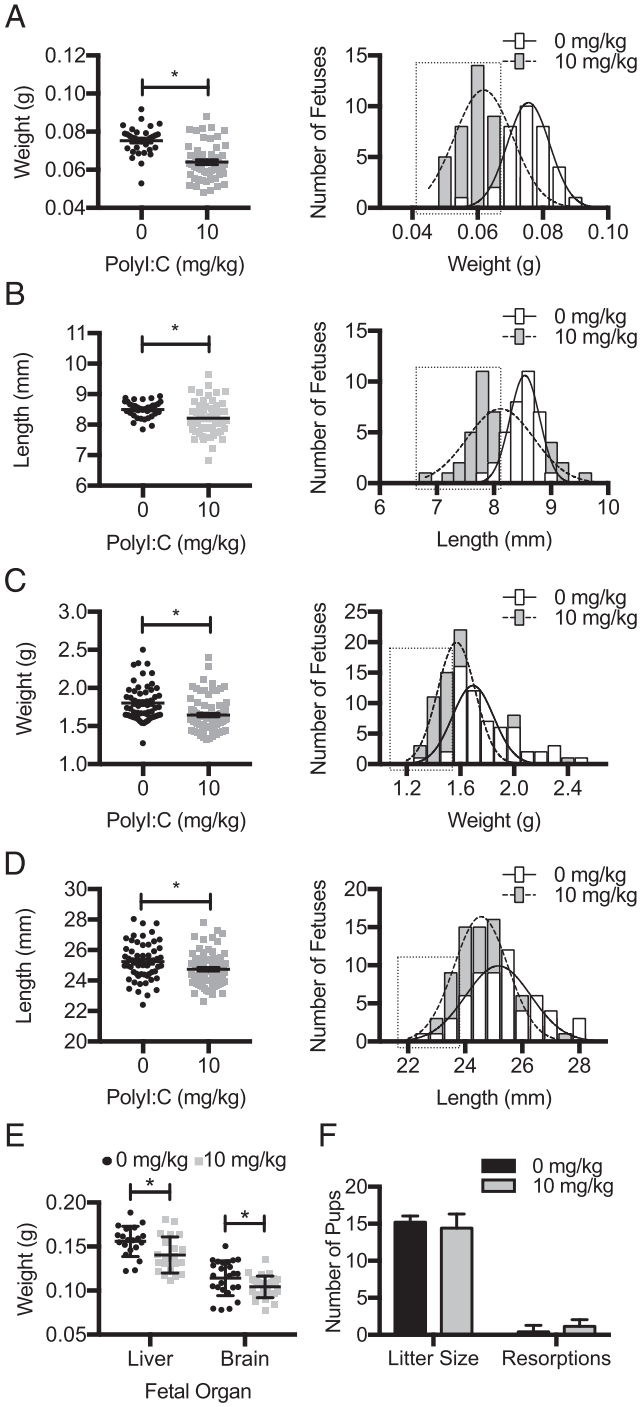

FIGURE 3. Maternal PolyI:C treatment early in pregnancy is associated with decreased fetal size at mid and late pregnancy. Following maternal administration of saline (0 mg/kg) or PolyI:C (10 mg/kg) on GD8.5, litters were collected on GD13.5 (**A**, **B**, and **F**) or GD18.5 (**C**–**E**). Fetal weight (A and C) and crown-rump length (B and D) were analyzed. (E) Fetal brain and liver weights were measured. (F) Litter size and number of resorptions are presented. Results represent means ± SEM. Data significantly different from controls ($p < 0.05$) are indicated by an asterisk (*) ($n = 35$ saline and $n = 53$ PolyI:C from at least six dams on GD13.5; $n = 58$ saline and $n = 81$ PolyI:C from at least six dams on GD18.5).

IFN-α promotes an antiviral response in rat TS cells and disrupts stem cell traits

PolyI:C is capable of directly inducing expression of genes associated with cellular antiviral responses. PolyI:C also robustly stimulates production of cytokines, such as type I IFNs and IL-6, which have pleiotropic effects on various cell types and mediate antiviral inflammation. Therefore, our next goal was to determine whether PolyI:C, type I IFNs, or IL-6 induce an antiviral response in TS cells. Treatment of rat TS cells with PolyI:C or IL-6 did not alter expression of genes associated with antiviral responses, including *Rsad2*, *Cxcl10*, *Irf7*, *Isg15*, and *Isg20*. Because some cell types only respond to PolyI:C if it is present within the cytosol (19), we transfected PolyI:C into rat TS cells but still did not observe any change in expression of these genes (data not shown). Likewise, exposure of rat TS cells to 100 U/ml IFN-γ (a type II IFN that is constitutively expressed in the conceptus during early pregnancy, owing to the prevalence of uterine NK cells) did not affect expression of any of these genes in TS cells. Conversely, exposure of rat TS cells to 100 U/ml IFN-α stimulated expression of *Cxcl10* (2.6-fold), *Rsad2* (7.1-fold), *Irf7* (11.6-fold), *Isg15* (24-fold), and *Isg20* (2-fold, Fig. 6A, all $p < 0.05$). In line with these results, robust expression of type I IFNR subunits *Ifnar1* and *Ifnar2* was detected in rat TS cells, whereas expression of IL-6R and the PolyI:C receptors *Tlr3* and *Ddx58* (which encodes RIG1) were low or undetectable (Fig. 6B). To further evaluate the responsiveness of TS cells to IFN-α, cells were exposed to low-dose (100 U/ml) or high-dose (1000 U/ml) IFN-α. IFN-α stimulated expression of *Cxcl10, Rsad2*, *Irf7*, and *Isg20* in a dose-dependent manner, with 1000 U/ml IFN-α increasing expression of these genes by 7.34-fold, 39-fold, 38-fold, and 2.97-fold, respectively. Both doses of IFN-α stimulated *Isg15* expression ~30-fold (Fig. 6C, $p < 0.05$).

After deducing that IFN-α stimulates an antiviral response in TS cells, our next goal was to determine whether IFN-α disrupts TS cell behavior. First, we evaluated proliferation in TS cells and found that there was no statistically significant change in proliferation as determined by percentage of cells that incorporated EdU (Fig. 7A, 7B) or that were positive for phospho-histone H3 (data not shown). We next evaluated expression of genes associated with maintaining the TS cell stem state and found that 1000 U/ml IFN-α decreased transcript levels of *Cdx2* (22%) and *Mest* (14%, Fig. 7C, $p < 0.05$). There was no statistically significant change in the expression of *Id2*. When TS cells were cultured in differentiation conditions, expression of the labyrinth-associated gene glial cells missing-1 (*Gcm1*) was increased by 5.3-fold, and the trophoblast giant cell–associated gene prolactin family 3, subfamily b, member 1 (*Prl3b1*; also called placental lactogen 2) was increased by 2.4-fold (Fig. 7D, both $p < 0.05$). However, in the presence of IFN-α, expression of *Gcm1* was reduced by 78%, and *Prl3b1* levels were reduced by 63% compared with cells not exposed to IFN-α (Fig. 7D, both $p < 0.05$). Thus, IFN-α disrupts expression of a subset of genes required to maintain TS cells in a stem state and inhibits their capacity to undergo differentiation into specialized trophoblast lineages.

Discussion

In this study, we show that maternal exposure to a viral stimulus during formation of the nascent placenta is associated with a robust antiviral response and hypoxia at the site of placental development, concomitant with reduced placental and fetal growth trajectories. We further found that TS cells express type I IFNR and respond to IFN-α by increasing IFN regulatory gene expression and decreasing expression of genes associated with the TS cell stem state. TS cells also exhibit impaired differentiation potential in the presence of IFN-α. Together, these results suggest that antiviral inflammation early in pregnancy impairs proper TS cell function and causes latent placental development and fetal growth.

Viral infections during pregnancy can result in a variety of perinatal outcomes. In some cases, a viral infection may have no

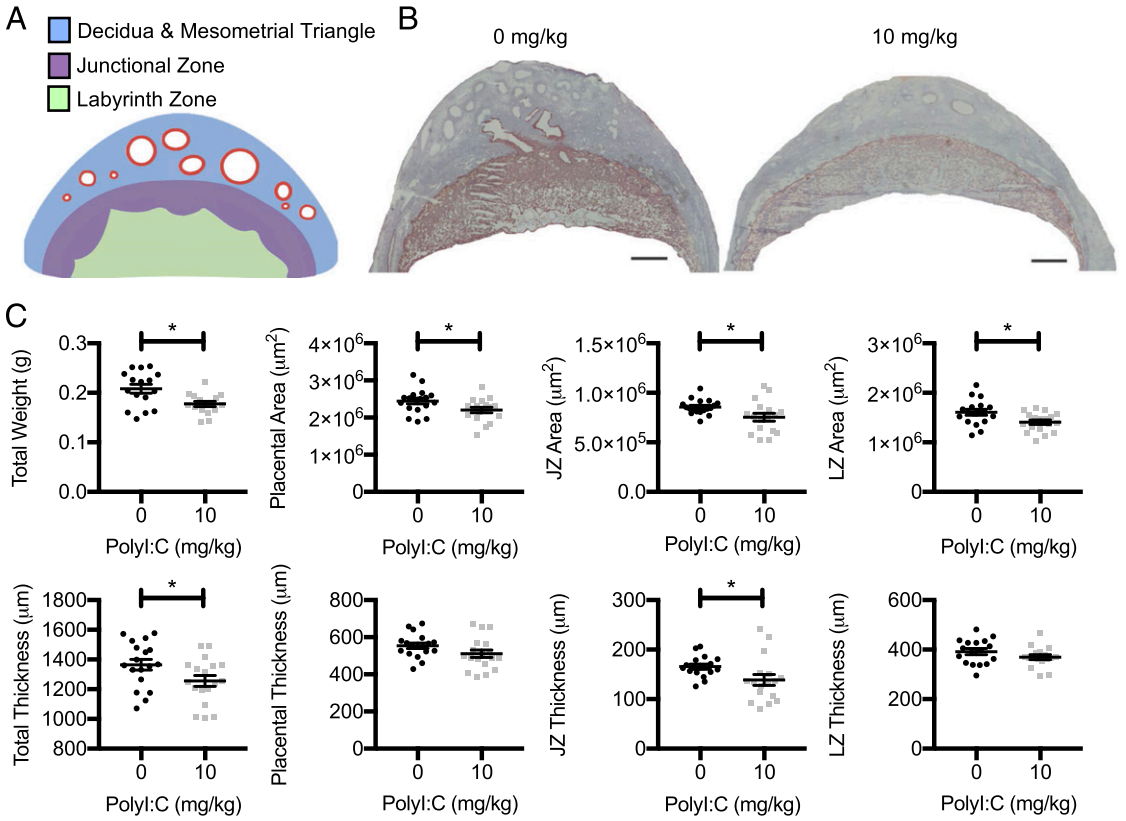

FIGURE 4. Changes in placental morphology and size following maternal PolyI:C exposure. (**A**) Schematic representation of a GD13.5 placenta. (**B**) Representative images of placentas collected on GD13.5 5 d after dams were injected with saline (0 mg/kg) or PolyI:C (10 mg/kg). Scale bar, 1000 μm. (**C**) Placentas were collected on GD13.5 and weighed, and sections were immunostained with vimentin to analyze area and thickness of the placenta, labyrinth zone (LZ), and junctional zone (JZ). Results represent means ± SEM. Data significantly different from controls ($n \geq 18$ placentas from six dams, $p < 0.05$) are indicated by an asterisk (*).

apparent effect on the health of a fetus or newborn, whereas in other cases, spontaneous abortion, FGR, or severe congenital anomalies may result. The different outcomes likely relate to the type of virus, the time during pregnancy when the infection is active, and whether the pathogen is transmitted to the fetus (such as with toxoplasmosis, other, rubella, CMV, and HSV infections, which are major causes of congenital anomalies) (33). Aside from toxoplasmosis, other, rubella, CMV, and HSV infections, the effect of viral inflammation on fetal and placental growth and development is poorly understood. Consequently, there is currently no standard of care for managing viral infections during pregnancy, despite the increased susceptibility of pregnant women to severe illness and mortality from viral infections (34). In this study, we sought to investigate the effect of viral inflammation on pregnancy outcome using the synthetic dsRNA molecule, PolyI:C. Because PolyI:C is a TLR3 ligand and robust stimulator of antiviral inflammation (19), the use of PolyI:C provides a means to elucidate the contribution of antiviral inflammation to pregnancy outcome in the absence of a pathogen. Previous studies have reported adverse pregnancy outcomes after administering PolyI:C to pregnant rodents, including embryonic lethality (18, 30, 35, 36), preeclampsia-like symptoms (5), preterm birth (37), and neurodevelopmental impairments in offspring (38). The novelty of our study is that we administered PolyI:C during early pregnancy prior to formation of the definitive placenta and then evaluated acute inflammation in the conceptus as well as placental and fetal growth throughout pregnancy. Because administration of PolyI:C to mice early in pregnancy results in embryonic lethality (18, 30, 35, 36), it was surprising that, in our hands, fetal viability was unaffected when rats were exposed to a similar dose per weight of PolyI:C, despite a robust antiviral response and hypoxia at the placentation site. Species differences in PolyI:C-TLR3 signaling responses have been reported (39), so these results may reveal differing susceptibility or sensitivity to PolyI:C between mice and rats. The use of rats may thus provide an advantage to study the effects of prenatal exposure to viral inflammation early in pregnancy on long-term placental function, fetal development, and offspring health without confounding embryonic demise. Our results that inflammation rather than viral burden affects early placental development and pregnancy outcome are consistent with other studies. For instance, exposure of pregnant immunocompetent mice to Zika virus early in pregnancy, prior to formation of the definitive placenta, causes placentation defects and adverse pregnancy outcomes despite rare detection of virus in the fetus or placenta. Interestingly, these adverse effects were limited to infection during early pregnancy and were less robust when the virus was administered at midpregnancy, when the placenta is functional (40). Thus, antiviral inflammation during early pregnancy may be a strong independent contributor to deficient placentation and adverse pregnancy outcomes regardless of pathogenic burden.

Proper fetal growth is an essential determinant of prenatal and perinatal health. Babies born growth restricted have a decreased chance of surviving their first year and have a higher risk of cardiovascular, metabolic, and neurodevelopmental sequelae in later life (10). FGR can be classified as symmetric (whole body) or asymmetric (head sparing). Asymmetric FGR is often due to extrinsic events (e.g., placental insufficiency, uterine anomalies) occurring late in pregnancy that cause more severe growth impairments in abdominal organs than the head. Symmetric FGR, in contrast, is usually attributed to an early embryonic event that

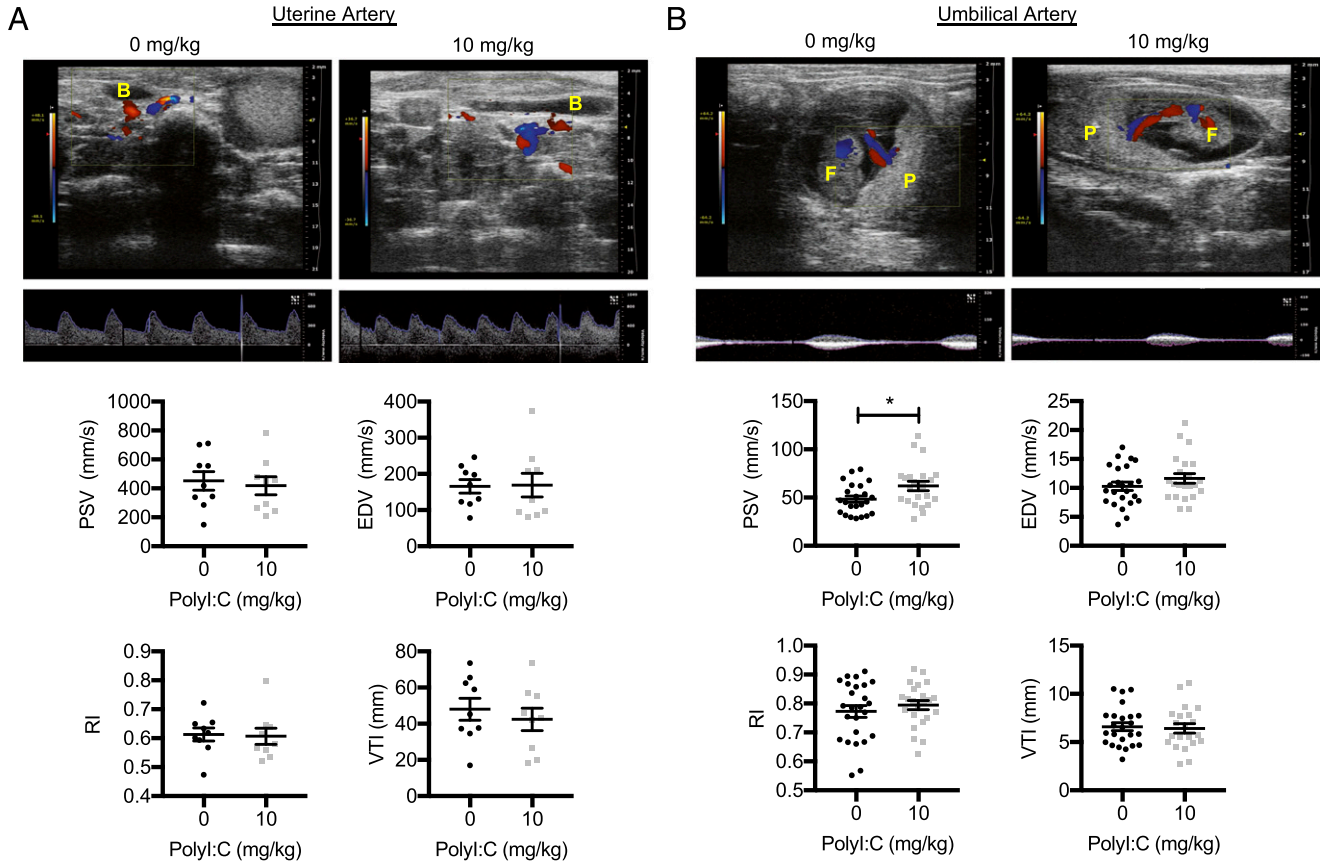

FIGURE 5. Effect of maternal PolyI:C exposure on uterine or umbilical artery blood flow. At GD13.5, 5 d after maternal exposure to saline (0 mg/kg) or PolyI:C (10 mg/kg), blood flow was evaluated by ultrasound biomicroscopy in uterine (**A**) and umbilical (**B**) arteries. VTI, PSV, and EDV were measured, and RI was calculated. Results represent means ± SEM. Data significantly different from controls ($n = 9$ dams for uterine artery, $n \geq 23$ fetuses from nine dams for umbilical artery, $p < 0.05$) are indicated by an asterisk (*). B, bladder; F, fetus; P, placenta.

causes all growth parameters to be below normal for gestational age. We observed that fetal weight was symmetrically decreased in later pregnancy when dams were exposed to PolyI:C during early gestation. We found no evidence of aberrant placental hemodynamics based on Doppler ultrasound recordings; thus, PolyI:C-induced FGR is unlikely to be attributed to alterations in placental blood flow dynamics. Therefore, viral inflammation reduced placental and fetal growth but did not impair placental hemodynamics, which are phenotypes consistent with symmetric FGR (41).

Viruses can be a major detriment to placental development. Viral infections have been associated with increased trophoblast apoptosis, decreased trophoblast invasion, production of proinflammatory responses, disruption of placental endocrine function, and increased risk of obstetric complications (42–46). Our findings using PolyI:C suggest that antiviral inflammation is sufficient to impair placentation and is consistent with other studies. For example, administration of PolyI:C to pregnant mice elicits maternal decidual leukocyte activation, decidual necroptosis, and production of TNF-α and IL-6 that induces STAT3 activation and endocrine disruption in placental cells (30, 31, 47). Prenatal PolyI:C exposure early in pregnancy also stimulates expression of IFN-induced transmembrane proteins, which interferes with trophoblast syncytialization and labyrinth zone formation, leading to embryo demise. Interestingly, mice lacking these transmembrane proteins are protected from PolyI:C-induced placental maldevelopment and embryonic loss, implicating placental maldevelopment as a critical determinant causing adverse pregnancy outcomes during viral inflammation (18). In rats, PolyI:C administration at midgestation is associated with altered expression of amino acid and drug transporters in the placenta, resulting in a corresponding change in amino acid concentrations in the fetus (48, 49). Term human placental explants also exhibit altered expression and function of multidrug resistance transporters following challenge with PolyI:C (50). In our study, we noted decreased expression of several maternally imprinted genes associated with placental and fetal growth after maternal PolyI:C exposure, including *Sfrp2, Dlk1,* and *Mest. Sfrp2* encodes a cysteine-rich protein that acts as a regulator of placental development through its modulation of the Wnt signaling pathway (51). *Dlk1* encodes a cell-surface transmembrane protein highly expressed in placental villi and exhibits reduced expression in FGR (52). *Mest* is expressed mainly by the placenta. Mice lacking *Mest* exhibit FGR because of a severe placental growth defect (53), and decreased expression of *Mest* is evident in human placentas during FGR (54). Our results are consistent with studies in which pregnant mice were challenged with a bacterial infection (*Campylobacter rectus*) early in pregnancy, resulting in FGR associated with repression of key developmental genes, including several imprinted genes (55, 56). Thus, it is possible that the latent fetal and placental growth observed after PolyI:C exposure is at least partially due to altered expression of key placental growth-promoting genes like *Mest.*

Recognition of dsRNA by pattern recognition receptors triggers an antiviral response that features synthesis of type I (α, β) IFNs. Type I IFNs are a family of 13 cytokines that bind to a single heterodimeric IFN-αR composed of two subunits, IFNAR1 and IFNAR2. Binding of type I IFNs to IFNAR initiates downstream signaling cascades that regulate activation and repression

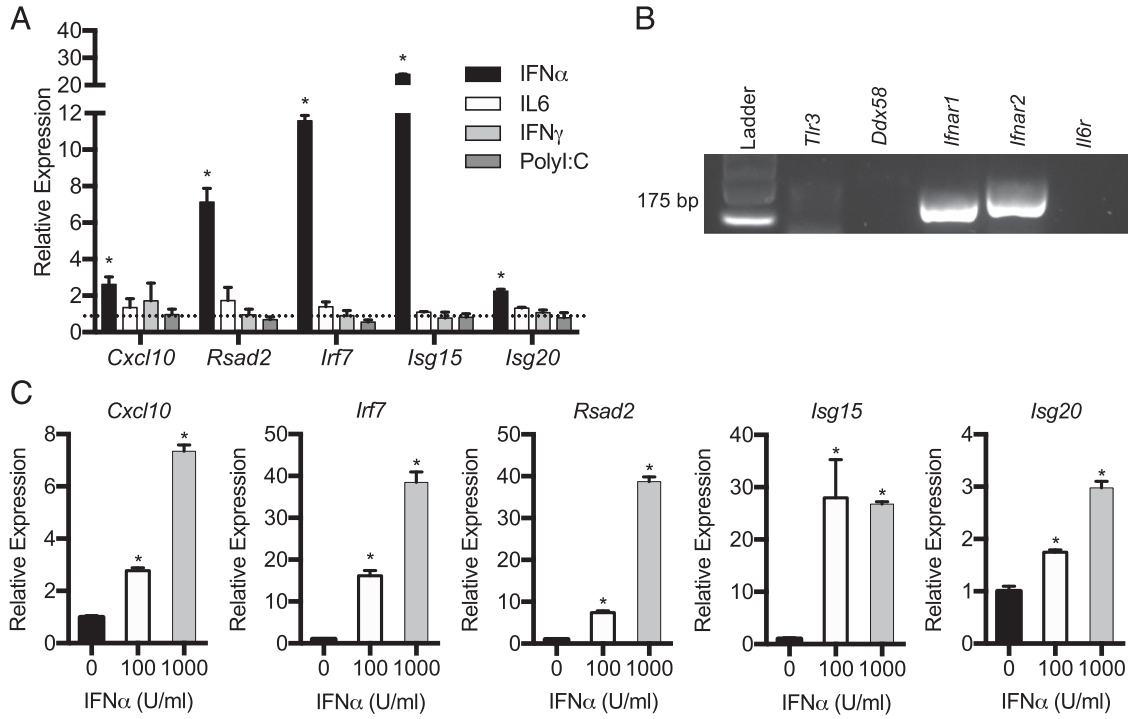

FIGURE 6. IFN-α promotes an antiviral response in rat TS cells. (**A**) Rat TS cells were exposed to 100 U/ml IFN-α, 20 ng/ml IL-6, 100 U/ml IFN-γ, and 50 μg/ml PolyI:C for 24 h. The expression of five representative antiviral genes (*Cxcl10*, *Rsad2*, *Irf7*, *Isg15*, and *Isg20*) was analyzed using qRT-PCR. Expression levels were calculated relative to five transcripts (*Rn18S, Ywhaz, Eef2, Gapdh, Actb*). The horizontal dotted line represents control rat TS cells that were not exposed to cytokines. (**B**) Expression of receptors that interact with PolyI:C (*Tlr3*, *Ddx58*), type I IFNs (*Ifnar1*, *Ifnar2*), and IL-6 (*Il6r)* were examined in rat TS cells by RT-PCR. (**C**) Rat TS cells were exposed to low-dose (100 U/ml) and high-dose (1000 U/ml) IFN-α, and expression of antiviral genes was assessed by qRT-PCR. Results represent means ± SEM. Data significantly different from controls ($n = 3$, $p < 0.05$) are indicated by an asterisk (*).

of hundreds of genes (57). The products of these genes promote a cellular antiviral state designed to limit replication and spread of viruses and other pathogens and can also alter cell proliferation, health, and viability in a cell-type and environment-specific context. The importance of type I IFNs for mediating systemic responses to viruses (and PolyI:C) in pregnant rodents is elegantly demonstrated in *Ifnar*$^{-/-}$ mice (36, 58, 59). Type I IFNs also alter stem cell traits in pluripotent and hematopoietic stem cells (60–62), so we postulated that type I IFNs impact TS cell behavior. We found that rat TS cells expressed high levels of *Ifnar1* and *Ifnar2* and robustly responded to IFN-α by increasing expression of various IFN-stimulated genes. IFN-α also decreased expression of genes associated with the TS cell stem state and placental growth, including *Mest*, and impaired their differentiation potential, as shown by reduced expression of *Gcm1* and *Prl3b1*. Thus, similar to reports with pluripotent and hematopoietic stem cells, type I IFN signaling may interfere with signal transduction pathways that maintain TS cell stem traits and temporarily disrupt normal TS cell function in the nascent placenta. Conversely, rat TS cells expressed low levels of *Tlr3, Ddx58,* and *Il6r*, and no detectable changes in IFN-stimulated genes were observed after rat TS cells were exposed to PolyI:C, IL-6, or to another IFN constitutively expressed at the placentation site, IFN-γ. These results are interesting because human and murine trophoblasts respond directly to PolyI:C, IL-6, and IFN-γ (63–65). Multiple cell types at the maternal-placental interface are capable of recognizing pathogen-associated molecular patterns, such as PolyI:C, and promote an antiviral state in part by producing type I IFNs. Our data suggest that TS cells are unable to recognize PolyI:C and some other inflammatory cytokines but possess the capacity to respond to type I IFNs. The narrow scope of TS cell responsiveness to viral patterns and cytokines other than type I IFNs may be a protective mechanism to avoid unwanted disruption of normal cellular functioning or viability while still contributing to an aggregate antiviral state. As they differentiate into specialized trophoblast lineages, trophoblasts may gain the capacity to recognize and respond to a broader range of immune mediators to limit pathogen replication and vertical transmission. Nonetheless, production of IFN-α in response to a viral infection early in pregnancy may be a determinant of acute changes in TS cell function, which could have long-lasting impacts on placental and fetal growth.

This study has several limitations. First, although humans and rats exhibit hemochorial placentation featuring regions with analogous structure and function (66), there are key differences in early placental development between these species. Therefore, we cannot conclude whether viral inflammation early in pregnancy affects human placental development in the same way as we observed for rat placentation. Of note, women diagnosed with primary CMV infection between 11 and 15 wk of pregnancy exhibit progressively increased placental thickness, as demonstrated through ultrasound examination (67), rather than decreased placental size, as would be suggested by our study. Potential explanations for this discrepancy are that CMV infection was detectable only after the placenta was formed and functional. In our study, the viral stimulus was provided during early placental development prior to chorioallantoic fusion. Thus, the timing of viral stimulus may be an important consideration. Moreover, the chronic CMV infection and relatively long duration of pregnancy in humans may have facilitated either a progressive edematous and inflammatory response or a placental compensatory response, resulting in a

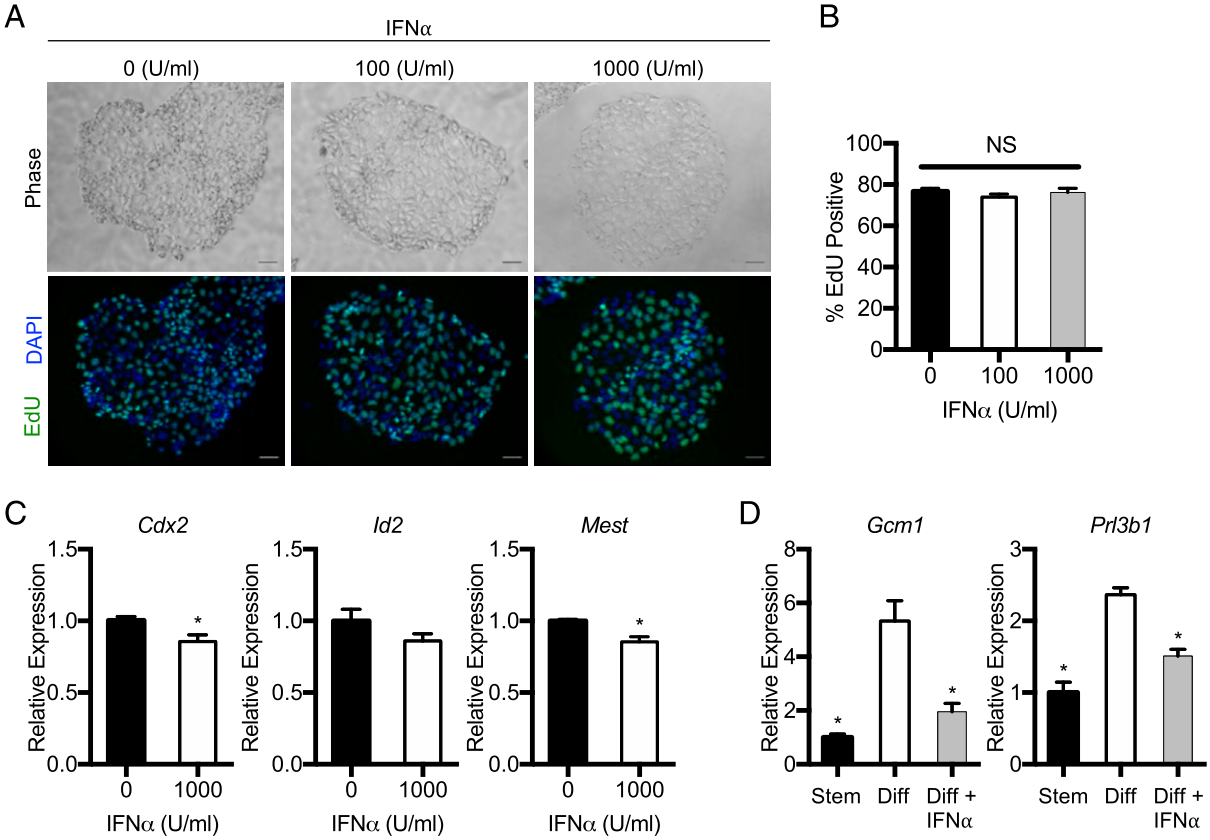

FIGURE 7. IFN-α inhibits expression of stem-related genes in rat TS cells. (**A**) Representative images of rat TS cells exposed to 1000 U/ml IFN-α. Proliferation of rat TS cells was evaluated by EdU incorporation. Scale bar, 50 μm. (**B**) Percentage of cells that incorporated EdU. (**C**) Expression of transcripts associated with TS cell stem state after rat TS cells were exposed to IFN-α for 24 h. (**D**) Expression of *Gcm1* and *Prl3b1* in rat TS cells following culture in stem conditions or in differentiation (Diff) conditions in the presence or absence of IFN-α. Data significantly different from controls [$n = 3$ for (A)–(C), $n = 4$ for (D); $p < 0.05$] are indicated by an asterisk (*).

thicker placenta that would not be apparent in our postmortem analyses in rats.

A second limitation is that we cannot ascertain that altered TS cell function in response to type I IFNs is directly responsible for the reduction in placental and fetal size after maternal PolyI:C. In future studies, these experiments could be performed using a line of rats in which the *Ifnar* gene is compromised by targeted genomic editing (68). Third, because PolyI:C was administered to dams systemically, we cannot conclude whether the concentration of dsRNA at the maternal-placental interface in our model represents the amount present within a typical virus infection. We attempted to evaluate the presence of dsRNA at the maternal-placental interface by immunofluorescence using a mAb (J2), but we were unable to detect robust staining. However, the profile of antiviral factors induced at the maternal-placental interface that was observed in our study is consistent with previous results that have used live viruses, such as Zika and influenza A (69–71), suggesting that the dose of PolyI:C used in our study elicits antiviral inflammation at the maternal-placental interface that is comparable to inflammation present during a virus infection.

Exposure of pregnant rodents to PolyI:C is frequently used as a model of brain maldevelopment and cognitive deficiencies in offspring (38), which is consistent with the known association between viral infections during pregnancy and increased risk of neurobehavioral impairments in humans (72). FGR is also an established risk factor for neurodevelopmental and behavioral problems in childhood (73). Thus, our findings provide a new dimension to the link between viral infections and FGR and raise the question of whether altered placental and fetal growth trajectories are causally linked to long-term neurobehavioral consequences. Our results may also help to stratify those pregnancies at risk for poor fetal growth following exposure to a viral infection by evaluating expression of genes associated with placental growth (e.g., *Mest)* so that targeted management strategies can be implemented to alleviate long-term health sequelae.

Acknowledgments

We thank Michael Soares for providing the rat TS cells.

Disclosures

The authors have no financial conflicts of interest.

References

1. Romero, R., F. Gotsch, B. Pineles, and J. P. Kusanovic. 2007. Inflammation in pregnancy: its roles in reproductive physiology, obstetrical complications, and fetal injury. *Nutr. Rev.* 65: S194–S202.
2. Cotechini, T., and C. H. Graham. 2015. Aberrant maternal inflammation as a cause of pregnancy complications: a potential therapeutic target? *Placenta* 36: 960–966.
3. Mor, G., I. Cardenas, V. Abrahams, and S. Guller. 2011. Inflammation and pregnancy: the role of the immune system at the implantation site. *Ann. N. Y. Acad. Sci.* 1221: 80–87.
4. Renaud, S. J., T. Cotechini, J. S. Quirt, S. K. Macdonald-Goodfellow, M. Othman, and C. H. Graham. 2011. Spontaneous pregnancy loss mediated by abnormal maternal inflammation in rats is linked to deficient uteroplacental perfusion. *J. Immunol.* 186: 1799–1808.
5. Chatterjee, P., L. E. Weaver, K. M. Doersch, S. E. Kopriva, V. L. Chiasson, S. J. Allen, A. M. Narayanan, K. J. Young, K. A. Jones, T. J. Kuehl, and B. M. Mitchell. 2012. Placental Toll-like receptor 3 and Toll-like receptor 7/8 activation contributes to preeclampsia in humans and mice. *PLoS One* 7: e41884.
6. Cotechini, T., M. Komisarenko, A. Sperou, S. Macdonald-Goodfellow, M. A. Adams, and C. H. Graham. 2014. Inflammation in rat pregnancy inhibits spiral artery

remodeling leading to fetal growth restriction and features of preeclampsia. *J. Exp. Med.* 211: 165–179.
7. Bakos, J., R. Duncko, A. Makatsori, Z. Pirnik, A. Kiss, and D. Jezova. 2004. Prenatal immune challenge affects growth, behavior, and brain dopamine in offspring. *Ann. N. Y. Acad. Sci.* 1018: 281–287.
8. 2019. ACOG practice bulletin no. 204: fetal growth restriction. *Obstet. Gynecol.* 133: e97–e109.
9. Brodsky, D., and H. Christou. 2004. Current concepts in intrauterine growth restriction. *J. Intensive Care Med.* 19: 307–319.
10. Sharma, D., S. Shastri, and P. Sharma. 2016. Intrauterine growth restriction: antenatal and postnatal aspects. *Clin. Med. Insights. Pediatr.* 10: 67–83.
11. Raghupathy, R., M. Al-Azemi, and F. Azizieh. 2012. Intrauterine growth restriction: cytokine profiles of trophoblast antigen-stimulated maternal lymphocytes. *Clin. Dev. Immunol.* 2012: 734865.
12. Sibley, C. P., P. Brownbill, M. Dilworth, and J. D. Glazier. 2010. Review: adaptation in placental nutrient supply to meet fetal growth demand: implications for programming. *Placenta* 31(Suppl.): S70–S74.
13. Baines, K. J., and S. J. Renaud. 2017. Transcription factors that regulate trophoblast development and function. *Prog. Mol. Biol. Transl. Sci.* 145: 39–88.
14. Soares, M. J., K. M. Varberg, and K. Iqbal. 2018. Hemochorial placentation: development, function, and adaptations. *Biol. Reprod.* 99: 196–211.
15. Ain, R., L. N. Canham, and M. J. Soares. 2003. Gestation stage-dependent intrauterine trophoblast cell invasion in the rat and mouse: novel endocrine phenotype and regulation. *Dev. Biol.* 260: 176–190.
16. Athanassakis, I., L. Papadimitriou, G. Bouris, and S. Vassiliadis. 2000. Interferon-γ induces differentiation of ectoplacental cone cells to phenotypically distinct trophoblasts. *Dev. Comp. Immunol.* 24: 663–672.
17. Hoshida, M. S., R. Gorjão, C. Lima, S. Daher, R. Curi, and E. Bevilacqua. 2007. Regulation of gene expression in mouse trophoblast cells by interferon-gamma. *Placenta* 28: 1059–1072.
18. Buchrieser, J., S. A. Degrelle, T. Couderc, Q. Nevers, O. Disson, C. Manet, D. A. Donahue, F. Porrot, K.-H. Hillion, E. Perthame, et al. 2019. IFITM proteins inhibit placental syncytiotrophoblast formation and promote fetal demise. *Science* 365: 176–180.
19. Palchetti, S., D. Starace, P. De Cesaris, A. Filippini, E. Ziparo, and A. Riccioli. 2015. Transfected poly(I:C) activates different dsRNA receptors, leading to apoptosis or immunoadjuvant response in androgen-independent prostate cancer cells. *J. Biol. Chem.* 290: 5470–5483.
20. Zavitsanou, K., C. K. Lim, T. Purves-Tyson, T. Karl, M. Kassiou, S. D. Banister, G. J. Guillemin, and C. S. Weickert. 2014. Effect of maternal immune activation on the kynurenine pathway in preadolescent rat offspring and on MK801-induced hyperlocomotion in adulthood: amelioration by COX-2 inhibition. *Brain Behav. Immun.* 41: 173–181.
21. Meyer, U., J. Feldon, M. Schedlowski, and B. K. Yee. 2005. Towards an immunoprecipitated neurodevelopmental animal model of schizophrenia. *Neurosci. Biobehav. Rev.* 29: 913–947.
22. Stridh, L., A. Mottahedin, M. E. Johansson, R. C. Valdez, F. Northington, X. Wang, and C. Mallard. 2013. Toll-like receptor-3 activation increases the vulnerability of the neonatal brain to hypoxia-ischemia. *J. Neurosci.* 33: 12041–12051.
23. Wang, A., S. D. Pope, J. S. Weinstein, S. Yu, C. Zhang, C. J. Booth, and R. Medzhitov. 2019. Specific sequences of infectious challenge lead to secondary hemophagocytic lymphohistiocytosis-like disease in mice. *Proc. Natl. Acad. Sci. USA* 116: 2200–2209.
24. Forrest, C. M., O. S. Khalil, M. Pisar, R. A. Smith, L. G. Darlington, and T. W. Stone. 2012. Prenatal activation of Toll-like receptors-3 by administration of the viral mimetic poly(I:C) changes synaptic proteins, N-methyl-D-aspartate receptors and neurogenesis markers in offspring. *Mol. Brain* 5: 22.
25. Schneider, C. A., W. S. Rasband, and K. W. Eliceiri. 2012. NIH Image to ImageJ: 25 years of image analysis. *Nat. Methods* 9: 671–675.
26. Asanoma, K., M. A. K. Rumi, L. N. Kent, D. Chakraborty, S. J. Renaud, N. Wake, D.-S. Lee, K. Kubota, and M. J. Soares. 2011. FGF4-dependent stem cells derived from rat blastocysts differentiate along the trophoblast lineage. *Dev. Biol.* 351: 110–119.
27. Stirnweiss, A., A. Ksienzyk, K. Klages, U. Rand, M. Grashoff, H. Hauser, and A. Kröger. 2010. IFN regulatory factor-1 bypasses IFN-mediated antiviral effects through viperin gene induction. *J. Immunol.* 184: 5179–5185.
28. Wenta, N., H. Strauss, S. Meyer, and U. Vinkemeier. 2008. Tyrosine phosphorylation regulates the partitioning of STAT1 between different dimer conformations. *Proc. Natl. Acad. Sci. USA* 105: 9238–9243.
29. Piedrahita, J. A. 2011. The role of imprinted genes in fetal growth abnormalities. Birth Defects Res. A. Clin. Mol. Teratol. 91: 682–692.
30. Thaxton, J. E., T. Nevers, E. O. Lippe, S. M. Blois, S. Saito, and S. Sharma. 2013. NKG2D blockade inhibits poly(I:C)-triggered fetal loss in wild type but not in IL-10$^{-/-}$ mice. *J. Immunol.* 190: 3639–3647.
31. Hsiao, E. Y., and P. H. Patterson. 2011. Activation of the maternal immune system induces endocrine changes in the placenta via IL-6. *Brain Behav. Immun.* 25: 604–615.
32. Kessous, R., B. Aricha-Tamir, A. Y. Weintraub, E. Sheiner, and R. Hershkovitz. 2014. Umbilical artery peak systolic velocity measurements for prediction of perinatal outcome among IUGR fetuses. *J. Clin. Ultrasound* 42: 405–410.
33. Silasi, M., I. Cardenas, J.-Y. Kwon, K. Racicot, P. Aldo, and G. Mor. 2015. Viral infections during pregnancy. *Am. J. Reprod. Immunol.* 73: 199–213.
34. Kourtis, A. P., J. S. Read, and D. J. Jamieson. 2014. Pregnancy and infection. *N. Engl. J. Med.* 370: 2211–2218.
35. Lin, Y., Y. Zeng, S. Zeng, and T. Wang. 2006. Potential role of toll-like receptor 3 in a murine model of polyinosinic-polycytidylic acid-induced embryo resorption. *Fertil. Steril.* 85(Suppl. 1): 1125–1129.
36. Yockey, L. J., K. A. Jurado, N. Arora, A. Millet, T. Rakib, K. M. Milano, A. K. Hastings, E. Fikrig, Y. Kong, T. L. Horvath, et al. 2018. Type I interferons instigate fetal demise after Zika virus infection. *Sci. Immunol.* 3: eaao1680.
37. Ilievski, V., S.-J. Lu, and E. Hirsch. 2007. Activation of toll-like receptors 2 or 3 and preterm delivery in the mouse. *Reprod. Sci.* 14: 315–320.
38. Reisinger, S., D. Khan, E. Kong, A. Berger, A. Pollak, and D. D. Pollak. 2015. The poly(I:C)-induced maternal immune activation model in preclinical neuropsychiatric drug discovery. *Pharmacol. Ther.* 149: 213–226.
39. Lundberg, A. M., S. K. Drexler, C. Monaco, L. M. Williams, S. M. Sacre, M. Feldmann, and B. M. Foxwell. 2007. Key differences in TLR3/poly I:C signaling and cytokine induction by human primary cells: a phenomenon absent from murine cell systems. *Blood* 110: 3245–3252.
40. Szaba, F. M., M. Tighe, L. W. Kummer, K. G. Lanzer, J. M. Ward, P. Lanthier, I.-J. Kim, A. Kuki, M. A. Blackman, S. J. Thomas, and J.-S. Lin. 2018. Zika virus infection in immunocompetent pregnant mice causes fetal damage and placental pathology in the absence of fetal infection. *PLoS Pathog.* 14: e1006994.
41. Fleiss, B., F. Wong, F. Brownfoot, I. K. Shearer, O. Baud, D. W. Walker, P. Gressens, and M. Tolcos. 2019. Knowledge gaps and emerging research areas in intrauterine growth restriction-associated brain injury. *Front. Endocrinol. (Lausanne)* 10: 188.
42. Griffiths, P. D., and C. Baboonian. 1984. A prospective study of primary cytomegalovirus infection during pregnancy: final report. *Br. J. Obstet. Gynaecol.* 91: 307–315.
43. Liu, T., X. Zheng, Q. Li, J. Chen, Z. Yin, J. Xiao, D. Zhang, W. Li, Y. Qiao, and S. Chen. 2015. Role of human cytomegalovirus in the proliferation and invasion of extravillous cytotrophoblasts isolated from early placentae. *Int. J. Clin. Exp. Med.* 8: 17248–17260.
44. Chou, D., Y. Ma, J. Zhang, C. McGrath, and S. Parry. 2006. Cytomegalovirus infection of trophoblast cells elicits an inflammatory response: a possible mechanism of placental dysfunction. *Am. J. Obstet. Gynecol.* 194: 535–541.
45. Arechavaleta-Velasco, F., Y. Ma, J. Zhang, C. M. McGrath, and S. Parry. 2006. Adeno-associated virus-2 (AAV-2) causes trophoblast dysfunction, and placental AAV-2 infection is associated with preeclampsia. *Am. J. Pathol.* 168: 1951–1959.
46. Miner, J. J., B. Cao, J. Govero, A. M. Smith, E. Fernandez, O. H. Cabrera, C. Garber, M. Noll, R. S. Klein, K. K. Noguchi, et al. 2016. Zika virus infection during pregnancy in mice causes placental damage and fetal demise. *Cell* 165: 1081–1091.
47. Yu, S.-X., F.-H. Zhou, W. Chen, G.-M. Jiang, C.-T. Du, G.-Q. Hu, Z.-Z. Liu, S.-Q. Yan, J.-M. Gu, X.-M. Deng, et al. 2017. Decidual stromal cell necroptosis contributes to polyinosinic-polycytidylic acid-triggered abnormal murine pregnancy. *Front. Immunol.* 8: 916.
48. McColl, E. R., and M. Piquette-Miller. 2019. Poly(I:C) alters placental and fetal brain amino acid transport in a rat model of maternal immune activation. *Am. J. Reprod. Immunol.* 81: e13115.
49. Petrovic, V., and M. Piquette-Miller. 2010. Impact of polyinosinic/polycytidylic acid on placental and hepatobiliary drug transporters in pregnant rats. *Drug Metab. Dispos.* 38: 1760–1766.
50. Lye, P., E. Bloise, M. Javam, W. Gibb, S. J. Lye, and S. G. Matthews. 2015. Impact of bacterial and viral challenge on multidrug resistance in first- and third-trimester human placenta. *Am. J. Pathol.* 185: 1666–1675.
51. Guilleret, I., M.-C. Osterheld, R. Braunschweig, V. Gastineau, S. Taillens, and J. Benhattar. 2009. Imprinting of tumor-suppressor genes in human placenta. *Epigenetics* 4: 62–68.
52. Wylie, A. A., S. K. Murphy, T. C. Orton, and R. L. Jirtle. 2000. Novel imprinted DLK1/GTL2 domain on human chromosome 14 contains motifs that mimic those implicated in IGF2/H19 regulation. *Genome Res.* 10: 1711–1718.
53. Lefebvre, L., S. Viville, S. C. Barton, F. Ishino, E. B. Keverne, and M. A. Surani. 1998. Abnormal maternal behaviour and growth retardation associated with loss of the imprinted gene Mest. *Nat. Genet.* 20: 163–169.
54. McMinn, J., M. Wei, Y. Sadovsky, H. M. Thaker, and B. Tycko. 2006. Imprinting of PEG1/MEST isoform 2 in human placenta. *Placenta* 27: 119–126.
55. Bobetsis, Y. A., S. P. Barros, D. M. Lin, R. M. Arce, and S. Offenbacher. 2010. Altered gene expression in murine placentas in an infection-induced intrauterine growth restriction model: a microarray analysis. *J. Reprod. Immunol.* 85: 140–148.
56. Bobetsis, Y. A., S. P. Barros, D. M. Lin, J. R. Weidman, D. C. Dolinoy, R. L. Jirtle, K. A. Boggess, J. D. Beck, and S. Offenbacher. 2007. Bacterial infection promotes DNA hypermethylation. *J. Dent. Res.* 86: 169–174.
57. Schreiber, G., and J. Piehler. 2015. The molecular basis for functional plasticity in type I interferon signaling. *Trends Immunol.* 36: 139–149.
58. Racicot, K., P. Aldo, A. El-Guindy, J.-Y. Kwon, R. Romero, and G. Mor. 2017. Cutting edge: fetal/placental type I IFN can affect maternal survival and fetal viral load during viral infection. *J. Immunol.* 198: 3029–3032.
59. Cappelletti, M., P. Presicce, M. J. Lawson, V. Chaturvedi, T. E. Stankiewicz, S. Vanoni, I. T. Harley, J. W. McAlees, D. A. Giles, M. E. Moreno-Fernandez, et al. 2017. Type I interferons regulate susceptibility to inflammation-induced preterm birth. *JCI Insight* 2: e91288.
60. Pietras, E. M., R. Lakshminarasimhan, J.-M. Techner, S. Fong, J. Flach, M. Binnewies, and E. Passegué. 2014. Re-entry into quiescence protects hematopoietic stem cells from the killing effect of chronic exposure to type I interferons. *J. Exp. Med.* 211: 245–262.
61. Smith, J. N. P., Y. Zhang, J. J. Li, A. McCabe, H. J. Jo, J. Maloney, and K. C. MacNamara. 2018. Type I IFNs drive hematopoietic stem and progenitor cell collapse via impaired proliferation and increased RIPK1-dependent cell death during shock-like ehrlichial infection. *PLoS Pathog.* 14: e1007234.
62. Eggenberger, J., D. Blanco-Melo, M. Panis, K. J. Brennand, and B. R. tenOever. 2019. Type I interferon response impairs differentiation potential of pluripotent stem cells. *Proc. Natl. Acad. Sci. USA* 116: 1384–1393.

63. Abrahams, V. M., T. M. Schaefer, J. V. Fahey, I. Visintin, J. A. Wright, P. B. Aldo, R. Romero, C. R. Wira, and G. Mor. 2006. Expression and secretion of antiviral factors by trophoblast cells following stimulation by the TLR-3 agonist, Poly(I: C). *Hum. Reprod.* 21: 2432–2439.
64. Jones, H. N., T. Jansson, and T. L. Powell. 2009. IL-6 stimulates system A amino acid transporter activity in trophoblast cells through STAT3 and increased expression of SNAT2. *Am. J. Physiol. Cell Physiol.* 297: C1228–C1235.
65. Hu, Y., R. Tan, C. D. MacCalman, G. Eastabrook, S.-H. Park, J. P. Dutz, and P. von Dadelszen. 2008. IFN-gamma-mediated extravillous trophoblast outgrowth inhibition in first trimester explant culture: a role for insulin-like growth factors. *Mol. Hum. Reprod.* 14: 281–289.
66. Soares, M. J., D. Chakraborty, M. A. Karim Rumi, T. Konno, and S. J. Renaud. 2012. Rat placentation: an experimental model for investigating the hemochorial maternal-fetal interface. *Placenta* 33: 233–243.
67. La Torre, R., G. Nigro, M. Mazzocco, A. M. Best, and S. P. Adler. 2006. Placental enlargement in women with primary maternal cytomegalovirus infection is associated with fetal and neonatal disease. *Clin. Infect. Dis.* 43: 994–1000.
68. Qaisar, N., S. Lin, G. Ryan, C. Yang, S. R. Oikemus, M. H. Brodsky, R. Bortell, J. P. Mordes, and J. P. Wang. 2017. A critical role for the type I interferon receptor in virus-induced autoimmune diabetes in rats. *Diabetes* 66: 145–157.
69. Bayer, A., N. J. Lennemann, Y. Ouyang, J. C. Bramley, S. Morosky, E. T. Marques, Jr., S. Cherry, Y. Sadovsky, and C. B. Coyne. 2016. Type III interferons produced by human placental trophoblasts confer protection against Zika virus infection. *Cell Host Microbe* 19: 705–712.
70. Steuerman, Y., M. Cohen, N. Peshes-Yaloz, L. Valadarsky, O. Cohn, E. David, A. Frishberg, L. Mayo, E. Bacharach, I. Amit, and I. Gat-Viks. 2018. Dissection of influenza infection in vivo by single-cell RNA sequencing. *Cell Syst.* 6: 679–691.e4.
71. Sheridan, M. A., D. Yunusov, V. Balaraman, A. P. Alexenko, S. Yabe, S. Verjovski-Almeida, D. J. Schust, A. W. Franz, Y. Sadovsky, T. Ezashi, and R. M. Roberts. 2017. Vulnerability of primitive human placental trophoblast to Zika virus. *Proc. Natl. Acad. Sci. USA* 114: E1587–E1596.
72. Kratimenos, P., and A. A. Penn. 2019. Placental programming of neuropsychiatric disease. *Pediatr. Res.* 86: 157–164.
73. Murray, E., M. Fernandes, M. Fazel, S. H. Kennedy, J. Villar, and A. Stein. 2015. Differential effect of intrauterine growth restriction on childhood neurodevelopment: a systematic review. *BJOG* 122: 1062–1072.